Overexpression of Metallothionein Reduces Diabetic Cardiomyopathy

Qiangrong Liang,[1] Edward C. Carlson,[2] Rajakumar V. Donthi,[3] Patrica M. Kralik,[3] Xia Shen,[3] and Paul N. Epstein[3]

Many diabetic patients suffer from cardiomyopathy, even in the absence of vascular disease. This diabetic cardiomyopathy predisposes patients to heart failure and mortality from myocardial infarction. Evidence from animal models suggests that reactive oxygen species play an important role in the development of diabetic cardiomyopathy. Our laboratory previously developed a transgenic mouse model with targeted overexpression of the antioxidant protein metallothionein (MT) in the heart. In this study we used MT-transgenic mice to test whether an antioxidant protein can reduce cardiomyopathy in the OVE26 transgenic model of diabetes. OVE26 diabetic mice exhibited cardiomyopathy characterized by significantly altered mRNA expression, clear morphological abnormalities, and reduced contractility under ischemic conditions. Diabetic hearts appeared to be under oxidative stress because they had significantly elevated oxidized glutathione (GSSG). Diabetic mice with elevated cardiac MT (called OVE26MT mice) were obtained by crossing OVE26 transgenic mice with MT transgenic mice. Hyperglycemia in OVE26MT mice was indistinguishable from hyperglycemia in OVE26 mice. Despite this, the MT transgene significantly reduced cardiomyopathy in diabetic mice: OVE26MT hearts showed more normal levels of mRNA and GSSG. Typically, OVE26MT hearts were found to be morphologically normal, and elevated MT improved the impaired ischemic contractility seen in diabetic hearts. These results demonstrate that cardiomyocyte-specific expression of an antioxidant protein reduces damage to the diabetic heart. *Diabetes* 51:174–181, 2002

A leading cause of death for diabetic patients is cardiac failure. Also, diabetic patients have an especially poor prognosis after myocardial infarction. Based on postmortem findings of heart failure in patients free of coronary artery disease or other known cardiac risk factors, Rubler et al. (1) first suggested the existence of a specific diabetic cardiomyopathy in 1972. Similar findings have been reported in other clinical studies (2,3). In addition, the increased risk of diabetic heart failure reported in the Framingham Heart Study (4) could not be explained by such diabetes-associated risk factors as obesity, hypertension, hypercholesterolemia, and coronary artery disease. Preclinical cardiac studies of diabetic patients (rev. in 5) have also reported left ventricular abnormalities independent of other risk factors. Together, these studies support the existence of a specific diabetic cardiomyopathy with origins in diabetic cardiac muscle.

Reactive oxygen species (ROS) have been proposed as a cause of many complications of diabetes (6,7). Hyperglycemia can elevate levels of ROS by increasing mitochondrial superoxide anion production (8,9) or by the process of glucose auto-oxidation (10). The heart is a susceptible target because it contains low levels of free radical scavengers (11). Available evidence implicating ROS in diabetic cardiomyopathy include increased cardiac lipid peroxidation (12,13) and elevated expression of genes for the antioxidants catalase (12,14,15) and heme oxygenase (16). Also, functional or morphological damage to diabetic hearts can be reduced with oral or systemic antioxidant administration (12,17). However, much of the current evidence lacks specificity. For example, the gene expression data are open to alternative interpretations because oxidative stress is not the only type of stress that can increase the activity of antioxidant genes. Also, the antioxidants that have been used to reduce cardiomyopathy lower circulating lipids (18,19), which may explain their beneficial actions in diabetic cardiomyopathy. Our laboratory has developed a transgenic model that expresses the potent antioxidant protein metallothionein (MT) specifically in cardiomyocytes. This model is ideal to test the significance of chronic ROS exposure because the transgene is overexpressed permanently and specifically in the heart.

RESEARCH DESIGN AND METHODS

Animals. We have previously described the development of OVE26 diabetic mice (20). MT mice that overexpress MT 10-fold in the heart were also previously described (21). Transgenic mice of both lines were identified by the presence of phenotypic markers. OVE26-positive mice were recognized by the presence of small eyes caused by the cointegration of the GR19 gene (20), which is expressed in the eye. MT-positive mice were recognized by the presence of coat color due to cointegration of the tyrosinase gene that corrects the mutant tyrosinase gene of FVB mice (22). All transgenic and nontransgenic animals were maintained on the inbred FVB background. Mice were maintained on a 12-h light/dark cycle and received food (Purina Laboratory Rodent Diet 5001) and water ad libitum. A U.S. Department of Agriculture–certified institutional animal care committee approved all animal procedures.

From the [1]Division of Molecular Cardiovascular Biology, University of Cincinnati, Ohio; the [2]Department of Anatomy and Cell Biology, University of North Dakota, Grand Forks, North Dakota; and the [3]Department of Pediatrics, University of Louisville, Louisville, Kentucky.

Address correspondence and reprint requests to Paul N. Epstein, Department of Pediatrics, University of Louisville, Baxter Research Building, Suite 321, Louisville, KY 40202. E-mail: paul.epstein@louisville.edu.

Received for publication 23 March 2001 and accepted in revised form 19 October 2001.

ANF, atrial natriuretic factor; GAPDH, glyceraldehyde 3-phosphate dehydrogenase; GSH, glutathione; GSSG, oxidized GSH; M2VP, 1-methyl-2-vinylpyridinium trifluoromethane sulfonate; MT, metallothionein; ROS, reactive oxygen species.

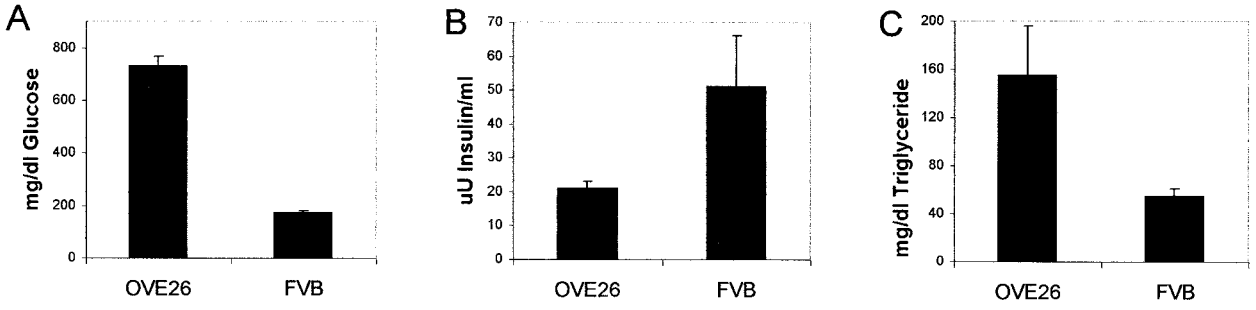

FIG. 1. Diabetes in OVE26 mice. Blood glucose (*A*), serum insulin (*B*), and serum triglycerides (*C*), measured as described in RESEARCH DESIGN AND METHODS, are shown. Values are from ad libitum–fed mice and show the mean ± SE for four to eight control or diabetic mice. In all panels, OVE26 values are different from control ($P < 0.05$ by Student's *t* test).

Glucose, insulin, triglyceride, and ketone assays. Glucose assays of fasted mice were performed with a Fast-Take (Lifescan) glucometer. Unfasted blood glucose values in OVE26 mice commonly exceeded the maximum of the glucometer and were assayed with a Sigma HK20 kit. Serum insulin levels were determined by double-antibody radioimmunoassay (16) using rat insulin (Eli Lilly) as standard. Serum triglycerides were determined by an automated method (Cobas Fara; Roche Diagnostic Systems). Plasma ketones were tested with Acetest Reagent Tablets (Bayer).

Reduced and oxidized glutathione. A Biooxytech GSH/GSSG-412 kit from Oxis Health Products was used to measure reduced and oxidized glutathione (GSSG). Hearts were homogenized in six volumes of 5% metaphosphoric acid with or without 33 mmol/l 1-methyl-2-vinyl-pyridinium trifluoromethane sulfonate (M2VP), a scavenger of reduced glutathione (GSH). The homogenate was centrifuged at 1,000*g* for 5 min. For GSH estimation, 5 μl supernatant was mixed with 355 μl assay buffer containing 100 mmol/l $NaPO_4$ and 5 mmol/l EDTA, pH 7.5. For GSSG estimation, 10 μl homogenate with M2VP was mixed with GSSG buffer containing 100 mmol/l $NaPO_4$ and 5 mmol/l EDTA, pH 10.05. The samples were mixed with 1.262 mmol/l 5,5′-dithiobis-(2-nitrobenzoic acid) and 15 units/ml GSH reductase. The mixture was incubated at room temperature for 5 min, and the absorbance was recorded at 412 nm for 3 min after the addition of 3.8 μmol NADPH.

RNA analysis. Northern blots were prepared as previously described (23) using 10 μg heart RNA from transgenic or control mice at 150 days of age. The membrane was prehybridized in 10 ml of Church buffer (1% bovine serum albumin, 7% SDS, 100 μg/ml salmon sperm DNA, and 0.5 mol/l NaH_2PO_4, pH 7.0) for 2 h. Then, the probe was added, and the blot was hybridized for 24 h. All procedures were carried out at 50°C. Oligonucleotide probes for mouse mRNAs for skeletal actin (TGGAGCAAAACAGAATGGCTGGCTTTAATGCT TCAAGTTTTCCATTTCCTTTCCACAGGG), atrial natriuretic factor (ANF; AATGTGACCAAGCTGCGTGACACACCACAAGGGCTTAGGATCTTTTGCGA TCTGCTCAAG), and glyceraldehyde 3-phosphate dehydrogenase (GAPDH) (GGAACATGTAGACCATGTAGTTGAGGTCAATGAAG) were labeled with [γ-^{32}P]ATP and polynucleotide kinase. The strength of the hybridization signal was determined on a Molecular Dynamics model 445 SI phosphoimager. Signals for skeletal actin and ANF were normalized to the signals for GAPDH.

Measurement of contractility. Cardiac contractility was measured in Langendorff mode by a modification of the method we previously described (24). In brief, the heart was retrogradely perfused with Krebs-Henseleit (KH) buffer (120 mmol/l NaCl, 20 mmol/l $NaHCO_3$, 4.6 mmol/l KCl, 1.2 mmol/l KH_2PO_4, 1.2 mmol/l $MgCl_2$, 1.25 mmol/l $CaCl_2$, and 11 mmol/l glucose). Hearts were paced throughout the procedure at 5 Hz (6V, 3 ms), which exceeded the spontaneous rates observed in our Langendorff preparations. Contractile force and heart rate are measured by means of an Grass FT03 force transducer hooked to the apex of the heart and connected to a ETH 400 bridge amplifier that fed into a Powerlab/400 amplifier. Once mounted, cardiac contractility was allowed to stabilize, which usually required 10–20 min. Baseline contractility was determined during the subsequent 30 min of recording. Next, the heart was subjected to a 60-min period of low-flow ischemia. This was achieved by switching a three-way valve to another perfusion line running from a buffer reservoir bubbled with 95% N_2 and 5% CO_2 to ensure hypoxia and a buffer pH of 7.4. The ischemic flow rate was 0.15 ml/min, which was one-tenth of the preischemia flow rate. For the last hour, the heart was again perfused with 95% O_2 and 5% CO_2–equilibrated KH buffer at 1.5 ml/min. Perfusion pressure, heart rate, contractile force, and the differential of force were continuously monitored. Data were analyzed using AD Instruments Chart for Windows version 3.3.5. Analysis of contractility during the ischemia and reperfusion periods was performed on the average of measurements made at 2-min intervals during the first 10 min of the period and at 10-min intervals for the remainder of the 60-min period. Basal contractility was determined from the average of measurements made at 10-min intervals throughout the 30-min basal period.

Electron microscopy. Fixation was carried out by vascular perfusion through the left ventricle. Mice were anesthetized with an intraperitoneal injection of pentobarbital (100 mg/kg). The right atrium was incised to allow exsanguination and fluid drainage. The perfusates included washouts (at 4°C) of 35 ml half-strength Karnovsky's (25) fixative with 1% procaine, and 75 ml full-strength Karnovsky's final fix. After perfusion, hearts were removed and immersed in chilled Karnovsky's fixative and then immediately cut transversely to produce ventricular "rings" (1- to 2-mm wide). The rings were minced to form small (1-mm^3) tissue blocks. Left ventricular tissue blocks were fixed at 4°C for 2–4 h. This was followed by rinsing in 0.2 mol/l sodium cacodylate buffer (pH. 7.4), postfixation in 1% OsO_4 (90 min), rinsing in distilled water, and en bloc staining in 0.5% aqueous uranyl acetate (90 min), all at 4°C. Dehydration proceeded through graded ethanols and propylene oxide. Tissue blocks were embedded in Epon/Araldite (26) and cured 48 h at 60°C. Epoxy blocks were trimmed, and 1-μm thick sections were made and stained with toluidine blue (1% in 1% sodium borate) for determination of tissue position and orientation. Thin sections were cut on an RMC MTXl ultramicrotome equipped with a Diatome diamond knife. Sections were collected on 300 mesh naked copper grids and stained with lead citrate (27) and uranyl acetate (4% in absolute ethanol). These were observed in a Hitachi 7500 transmission electron microscope at initial magnifications of 4,000–15,000 diameters.

To quantify the morphological features of cardiac tissues in each of the animal groups, transmission electron micrographs of randomly selected areas of left ventricular thin sections were printed at identical magnifications. Two observers who were unaware of their origin rated these prints. On a scale of 1–4, observers rated the morphology relative to a figure exhibiting near-perfect cardiac morphology. Figures were rated for overall morphology (which included the presence of edematous areas, myelin figures, and overall organization), mitochondrial morphology (which included mitochondrial packing, density, and shape), and myofilament morphology (which examined linearity of the *Z* lines, linearity of myofilaments, regularity of myofilaments, and continuity of myofilaments).

Statistical analysis. Statistical comparisons of GSH, RNA expression, and cardiac contractility were performed by one-way analysis of variance and Bonferroni's post hoc tests, unless otherwise indicated in the text. The significance of differences for morphology ratings were determined by the Kruskal-Wallis test followed by Dunn's multiple comparison test. Comparisons between two groups were performed with Student's *t* test.

RESULTS

Diabetes in OVE26 and OVE26MT transgenic mice. The transgenic line OVE26 was used to evaluate diabetic cardiomyopathy. As previously described (20), these mice exhibit very high blood glucose concentrations and reduced serum insulin values (Figs. 1*A* and *B*). Figure 1*C* also shows that OVE26 mice possess elevated serum triglycerides. Assays of seven diabetic plasma samples for the presence of ketones were negative (not shown). MT overexpression was produced in diabetic mice by crossing OVE26 mice with an MT transgenic line that we previously described (21) and that has a 10-fold increase in cardiac MT. Fasting blood glucose levels were measured to rule

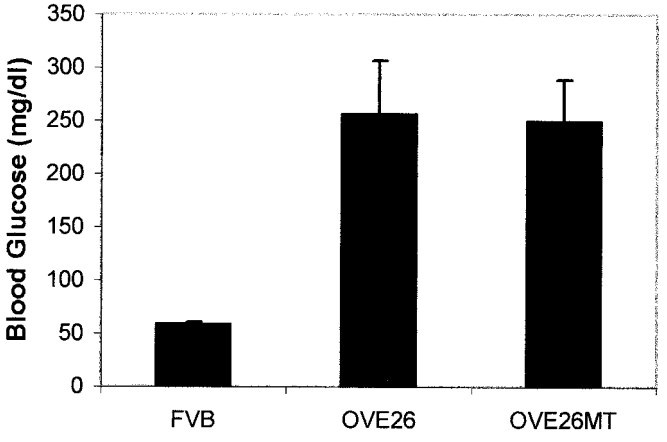

FIG. 2. Elevated blood glucose levels in OVE26 and OVE26MT mice. Fasted blood glucose values were determined as described in RESEARCH DESIGN AND METHODS. Both transgenic values are different from control ($P < 0.01$ by one way analysis of variance) and not significantly different from one another. Values are the mean ± SE for 8–10 control or transgenic mice.

out any effect of the MT transgene on diabetes. As shown in Fig. 2, OVE26 and OVE26MT mice had elevated and indistinguishable levels of hyperglycemia. Random assays of unfasted blood samples also demonstrated no effect of the MT transgene on glycemia (not shown).

Reduced GSH and GSSG in heart tissue. Conversion of GSH to GSSG is important for several endogenous antioxidant reactions, and the antioxidant properties of GSH and MT are both dependent on sulfhydryl groups. Therefore, we measured reduced GSH and GSSG to assess oxidative stress in diabetic hearts and to determine whether MT protects the heart from oxidative stress. GSH levels in OVE26 and OVE26MT hearts were similar to levels in control FVB hearts (Fig. 3). However, a significantly increased level of GSSG demonstrated oxidative stress in diabetic hearts. Importantly, the elevation in GSSG was completely eliminated in OVE26MT mice.

RNA levels. A common finding in cardiomyopathy is upregulation of mRNAs for skeletal actin and ANF. These transcripts were increased two- to threefold in the hearts of our OVE26 mice (Fig. 4), confirming a diabetes-induced cardiomyopathy. MT overexpression significantly reversed the increase in skeletal actin mRNA in hearts of OVE26MT mice. MT also reduced ANF expression, but this reduction did not reach significance. Failure to reach significance was partially caused by a high degree of variability in ANF expression, which has been observed by others (28).

Morphology. Morphological analyses of left ventricular cardiac tissues from three groups of mice ~150 days old were carried out by transmission electron microscopy (Fig. 5). Cardiomyocytes from control FVB mice (Fig. 5*A*) showed ultrastructural features considered typical for this cell type. In contrast, heart tissue from diabetic OVE26 animals (Fig. 5*B*) showed clearly the detrimental effects of the disease. Disorganized collections of mitochondria randomly interspersed between disrupted myofibrils in an edematous sarcoplasm were common. In addition, numerous myelin figures suggested membrane disruption and cellular damage in these tissues. Overexpression of MT had a striking protective effect against the myocardial injury seen in diabetic animals (Fig. 5*C*). In cardiomyocytes of OVE26MT animals, mitochondria and myofibrillar fine structure were essentially indistinguishable from FVB controls. Moreover, myelin figures and other evidence of myocardial injury were not seen. As described in RESEARCH DESIGN AND METHODS, semiquantitative ratings were made of random electron micrographs by observers blind to the origin of the picture. These figures were judged for overall morphology, mitochondrial structure, and myofibrillar substructure. Figure 5*D* shows that in this unbiased evaluation of morphology, the OVE26 diabetic group was significantly compromised relative to either of the other groups. This analysis also confirmed that MT was highly protective to the diabetic heart, because there were no significant differences between ultrastructural features of cardiomyocytes in FVB control and OVE26MT hearts.

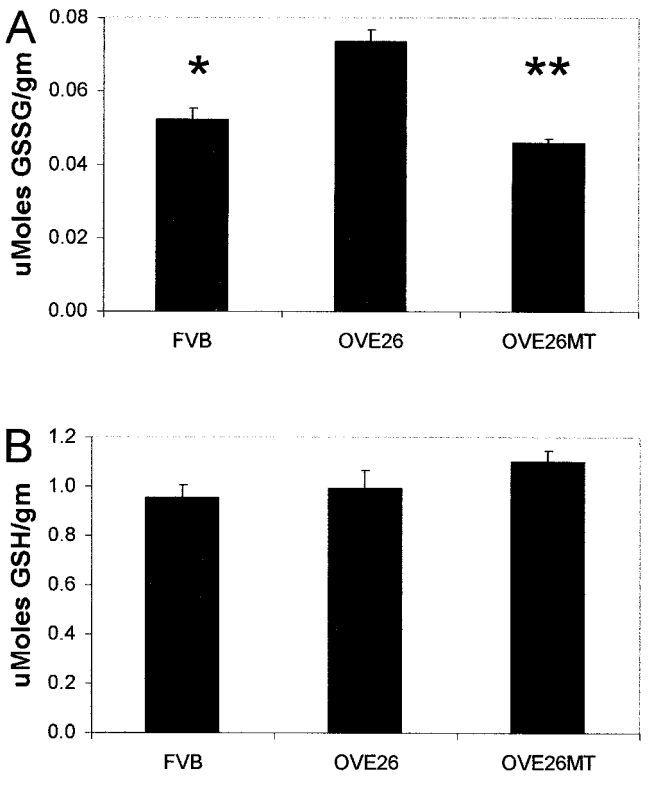

FIG. 3. MT overexpression prevents diabetes-induced increase in cardiac GSSG. Levels of cardiac GSSG (*A*) and GSH (*B*) were determined as described in RESEARCH DESIGN AND METHODS. Values are the mean ± SE for 8–10 control or transgenic mice. *Significantly different from OVE26 ($P < 0.05$); **also significantly different from OVE26 ($P < 0.01$).

Contractility. To assess the impact of diabetes and potential protection by MT overexpression, cardiac contractility was measured in Langendorff-perfused hearts (Fig. 6). During the basal period of perfusion, there was a trend toward reduced contractility in OVE26 and OVE26MT hearts, but this trend did not reach significance in either case. Under ischemic conditions, diabetes clearly reduced contractility in OVE26 hearts, and this deficit was strikingly reversed in OVE26MT hearts by MT overexpression. During the reperfusion phase, there was also a decrement in diabetic contractility compared with FVB hearts. This trend was not significant by the Bonferroni post hoc test. However, when this trend was tested with Dunnett's one-way post hoc test, all three parameters of contractility were significantly ($P < 0.05$) diminished in

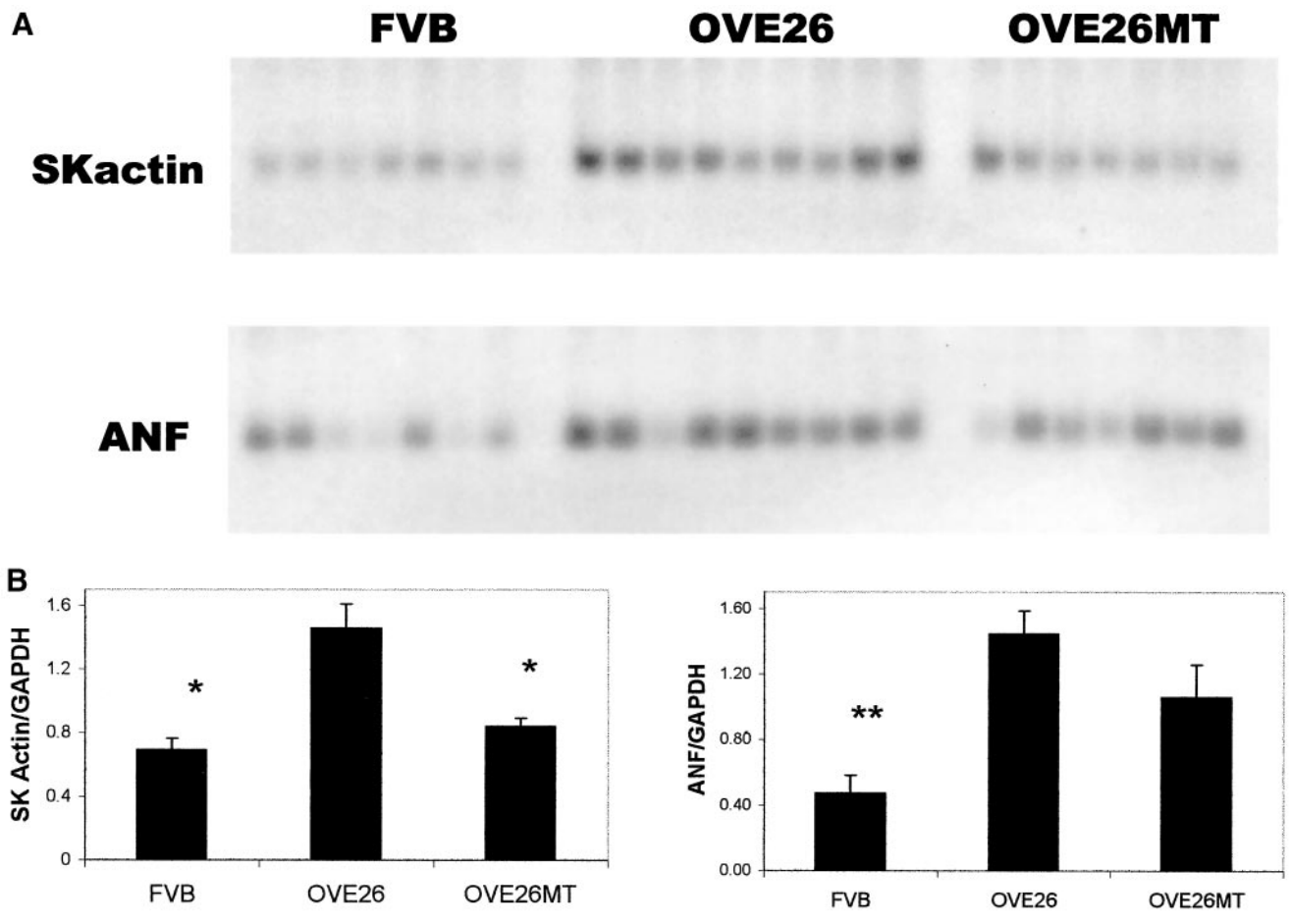

FIG. 4. MT overexpression prevents elevated skeletal actin mRNA expression in diabetic heart. *A*: Northern blot of FVB, OVE26, and OVE26MT cardiac RNA probed for skeletal actin and ANF mRNAs. *B*: Quantitation of the skeletal actin and ANF signals normalized to GAPDH mRNA. *Significantly different from OVE26 ($P < 0.01$); **significantly different from OVE26 and OVE26MT ($P < 0.05$). Vertical bars indicate the SE.

OVE26 hearts compared with FVB hearts. OVE26MT contractility was not significantly different from either of the two other groups during reperfusion, as assessed by either the Bonferroni test or the Dunnett test. Thus, it is not possible to determine from the present data whether MT has an effect on contractility during reperfusion.

DISCUSSION

Our results demonstrate obvious cardiomyopathy in OVE26 diabetic mice. Disruption of normal cardiac function was apparent as aberrant gene expression, disrupted cellular morphology, and decreased ischemic and reperfusion contractility. MT overexpression markedly reduced the degree of cardiac damage for each of these parameters, except for reperfusion contractility.

The OVE26 mouse has not been used extensively for the study of diabetes complications, despite the fact that this transgenic diabetic model was first described 12 years ago (20). Early onset, insulinopenic diabetes results from a transgene that overexpresses calmodulin only in pancreatic β-cells (20). The pathology of these animals has at least one feature similar to type 1 diabetes; hyperglycemia is a direct result of damage to the β-cell. However, unlike type 1 diabetes, this damage is not immune-mediated, and a low but significant level of insulin secretion is retained. These mice provide several advantages for the study of chronic cell and tissue damage resulting from diabetes: all OVE26 mice have a very consistent onset and severity of diabetes. Their duration of diabetes is long; they can live with diabetes for 2 years without insulin therapy. In these mice, diabetes is caused by a known genetic alteration whose direct actions are specific to the β-cell. Also, potential artifacts secondary to the use of diabetogenic chemicals such as streptozotocin and alloxan are avoided. However, despite these advantages for the study of complications, it is essential to recognize a major difference between OVE26 diabetes and human diabetes: the complications in humans develop in a much less severe diabetic environment because of insulin administration to these patients. Therefore, the findings identified in OVE26 mice should be replicated in milder models of diabetes, such as those inducible with diet (29). It would also be of value to confirm the protective value of MT overexpression in more widely used diabetic models, such as *db/db* and streptozotocin-induced diabetic mice.

Diabetic cardiomyopathy in the OVE26 mice is similar in most respects to the cardiomyopathy described in other diabetic models. Morphological damage comparable to what we observed in OVE26 mice has been reported in other models (12,30), and diabetes-induced changes in cardiac contractile gene expression have also been reported (31). In most studies of rodent diabetes, basal contractility was significantly reduced. In OVE26 mice, we only observed a trend toward reduced basal contractility.

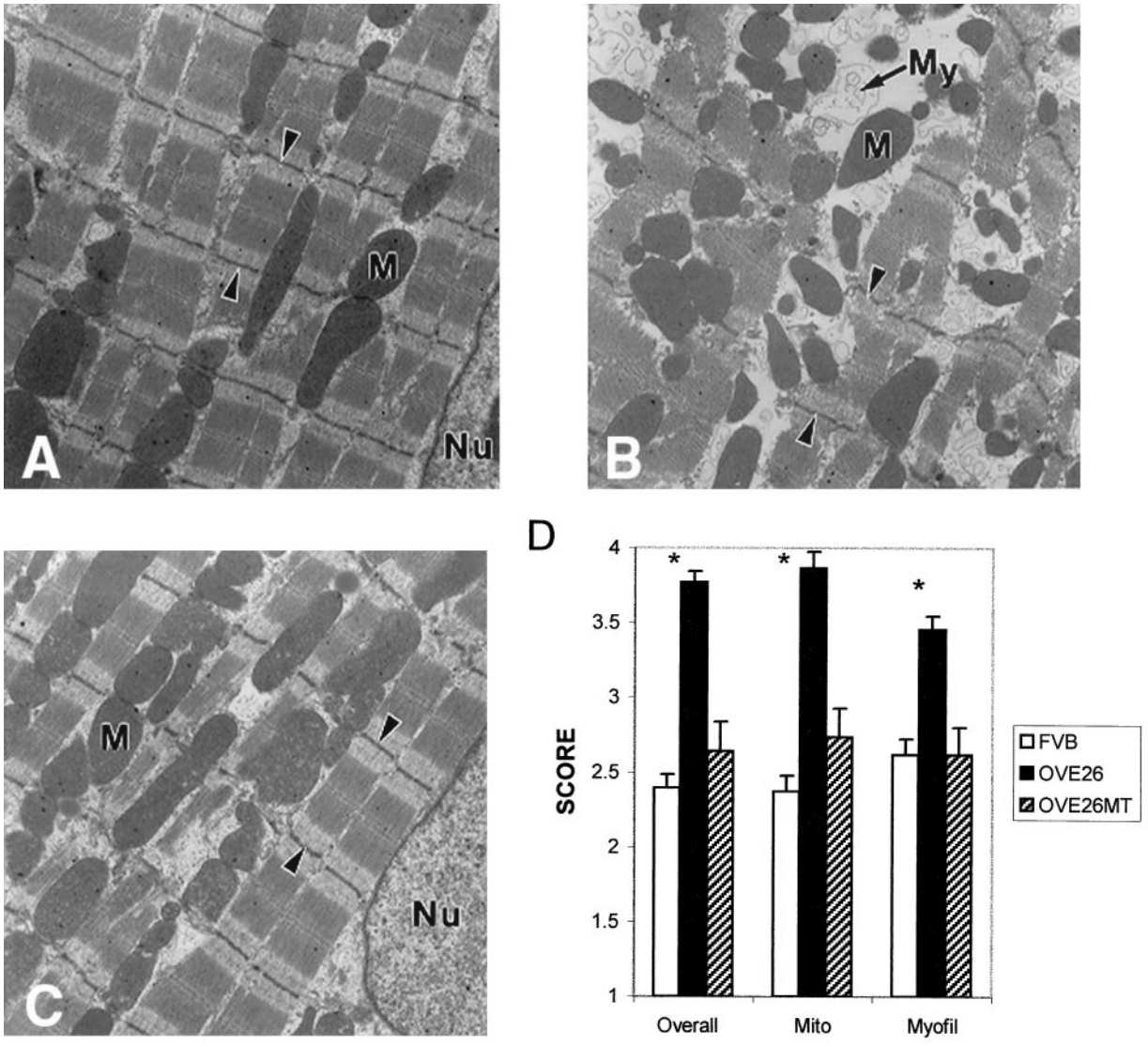

FIG. 5. *A* and *C*: MT overexpression protects cardiac morphology from chronic diabetes. Representative transmission electron micrographs of cardiac tissues from left ventricles of FVB (*A*), OVE26 (*B*), and OVE26MT (*C*) mice are shown. FVB and OVE26MT–cross animals (*A* and *C*) show normal myocardial fine structure, with myofibrils comprised of regular and continuous sarcomeres. The latter are demarcated by Z lines (arrowheads), which are in register with adjacent myofibrils. Rows of moderately electron dense mitochondria (M) intervene between myofibrils. OVE26 diabetic myocardium (*B*) shows randomly distributed mitochondria (M) between poorly organized myofibrils (arrowheads indicate Z lines) in an electron-lucent sarcoplasm. Numerous myelin figures (My) suggest myocardial cytopathology. All figures have a magnification of 8,500×. *D*: Quantitation of cardiac morphology. Two blind observers rated ultrastructural features of myocardial tissues in 16–25 randomly selected electron micrographs from each of three OVE26 diabetic mice, three OVE26MT mice, and three nontransgenic FVB control mice. The parameters used for the overall ratings and ratings for mitochondria (Mito) and myofilaments (Myofil) are described in RESEARCH DESIGN AND METHODS *OVE26 differs from OVE26MT and FVB ($P < 0.001$). Vertical bars indicate the SE.

However, this trend may reflect a real underlying defect in basal contractility, because we recently observed impaired basal contractility in isolated OVE26 cardiomyocytes (32). In the current study, diabetic contractility was more impaired during ischemia and reperfusion than in control animals. Increased sensitivity of cardiac contractility to ischemia has been described in other rodent models of diabetes (33). Our results show that the OVE26 mouse develops a cardiomyopathy that is suitable for testing other transgenes by simple breeding strategies. We used this strategy in the current study to demonstrate the benefit of MT overexpression.

MT was effective in reversing many aspects of diabetic cardiomyopathy. However, MT had little or no effect on the diabetic deficit in contractility seen during basal or reperfusion phases. The failure of MT to protect contractility under oxidative perfusion conditions raises the possibility that this component of failure may be caused by factors other than ROS. Indeed, many mechanisms other than ROS have been implicated in diabetic complications. For example, pyruvate dehydrogenase activity is markedly reduced in diabetic hearts (34). This may pose a serious disadvantage to the diabetic heart under our perfusion conditions, which used glucose as the sole energy source. Pyruvate dehydrogenase is essential for maximal ATP production from glucose under oxidative conditions. Because MT overexpression would not restore pyruvate dehydrogenase activity, this could contribute to the lack of benefit of MT on contractility during oxidative conditions.

Because the contractility data obtained in this study was

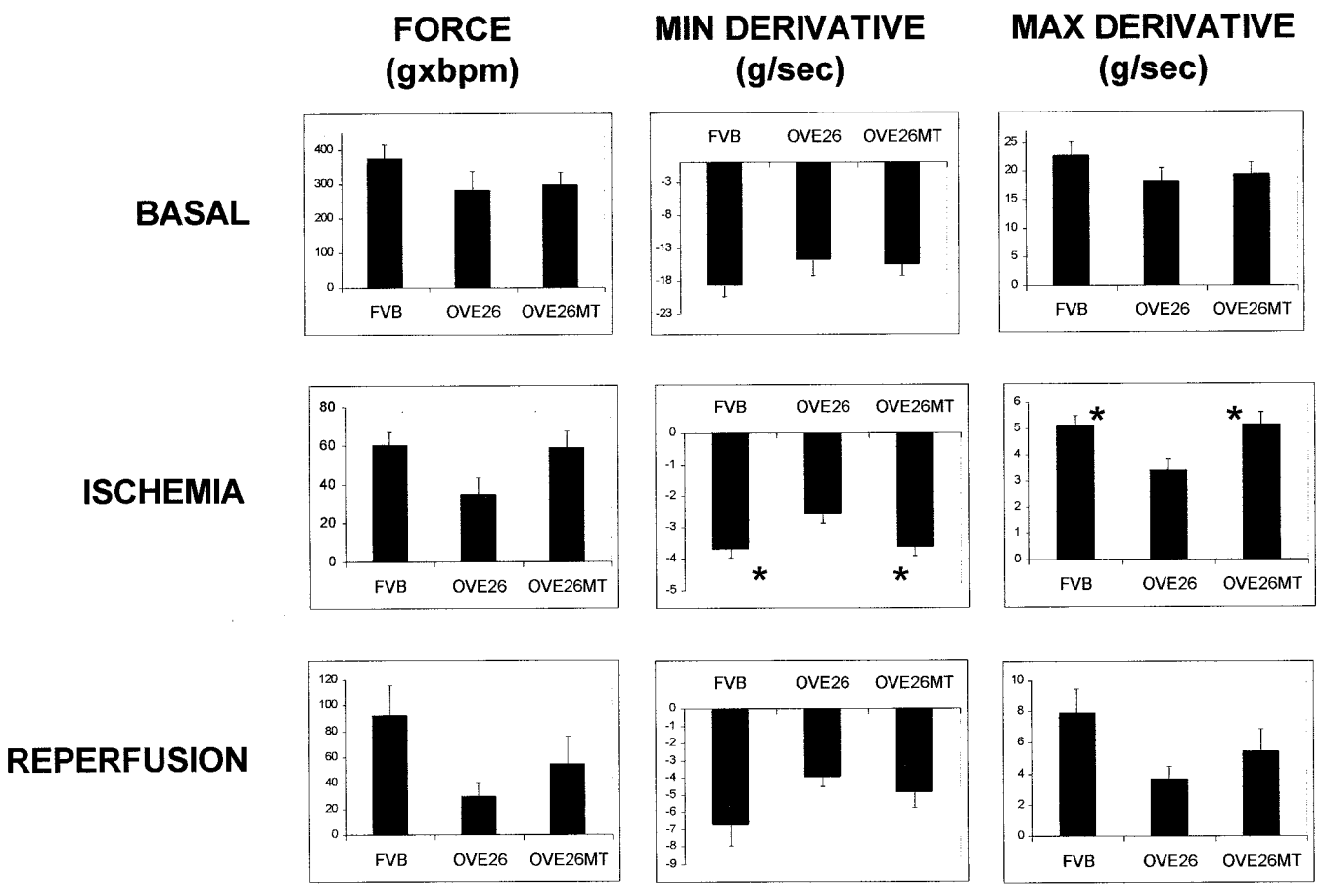

FIG. 6. MT overexpression blocks diabetes-induced reductions in ischemic contractility. Contractility was measured as force and the minimum (MIN) and maximum (MAX) derivatives of force during Langendorff perfusion, as described in RESEARCH DESIGN AND METHODS. Values are averages obtained over the entire basal, ischemic, or reperfusion period. For each group, n = 7–9. *Different from OVE26 values, $P \leq 0.05$. Vertical bars indicate the SE.

derived from Langendorff perfused hearts, extrapolation of these results to cardiac function in the whole diabetic animal should be made with caution. Unlike in the intact animal, Langendorff hearts perform little work. In addition, Langendorff as well as perfused working hearts beat at about half the rate of the normal mouse heart (35,36), are perfused with incomplete media, and demonstrate markedly decreased rates of pressure development (36). Sophisticated systems for analysis of cardiac function in vivo have been developed for the mouse (35,37). These systems provide a more realistic evaluation of normal and pathological function that should be applied to murine models of diabetic cardiomyopathy.

Disagreement exists over the question of whether diabetic cardiomyopathy is a direct effect of diabetes on the heart. Some propose that diabetic heart failure is secondary to vascular dysfunction (38,39). Decreased delivery of fuel and oxygen by the coronary circulation could result in cumulative damage to the heart. Our results show that direct manipulation of the cardiomyocyte can alter the course of diabetic cardiomyopathy. Because the α-myosin heavy chain promoter is active only in cardiomyocytes, and expression data confirm this in these transgenic mice (21,40), MT could not have exerted its protective actions in the vasculature by altering other components of diabetes. The fact that protection was obtained using a protein expressed exclusively in the cardiomyocyte confirms that diabetic cardiomyopathy is a pathology intrinsic to the myocyte.

Our results strengthen the hypotheses that diabetes increases oxidative stress in the heart, which contributes to diabetic cardiomyopathy. Prior studies using cardiac tissue or cardiomyocytes from animal models of diabetes demonstrated upregulation of antioxidant enzymes (14), increased production of hydrogen peroxide (41), and increased lipid peroxidation (12,13). Recently, oxidative stress in diabetic human hearts has been shown (42) by the finding of elevated levels of the marker of oxidative damage, nitrotyrosine, in biopsies from diabetic patients. In the current study, we demonstrated that GSSG is elevated in diabetic hearts. GSSG is produced by oxidation of GSH during several antioxidant reactions, including the detoxification of hydrogen peroxide by GSH peroxidase. To our knowledge it has not previously been shown that GSSG is increased in diabetic hearts. We saw no corresponding change in GSH concentration. This stability of GSH levels in diabetic hearts was not surprising because a 40% increase in GSSG would be expected to have little impact on GSH, which was present in 20-fold excess. Other authors have also examined GSH in diabetic hearts (43,44) and found it to be unaltered.

Overexpression of MT was effective in both preventing the diabetes-induced change in GSSG levels and reducing several components of diabetic cardiomyopathy. MT has

been shown to defend against many agents known to act through ROS, including radiation, GSH depletors, and xanthine oxidase (rev. in 45,46). The antioxidant action of MT is 50–100 times greater than GSH on a molar basis (47,48). In the current transgenic model, Kang and colleagues (21,49) have also shown that MT protects the heart from ROS damage caused by doxorubicin and hydrogen peroxide. Because ROS damage is prominent in experimental (12) and clinical (42) samples of diabetic hearts, it is likely that the antioxidant actions of MT are the source of the protection demonstrated for morphology, gene expression, and ischemic contractility. These results support continued efforts to find an antioxidant regimen effective for the prevention of cardiac complications of diabetes.

ACKNOWLEDGMENTS

This study was supported by the Commonwealth of Kentucky Research Challenge Trust Fund and grants HL62892 and HL66778.

The authors thank Dr. Kap Lee for expert help in animal health and surgery and Janice Audette for excellent technical assistance in electron microscopy.

REFERENCES

1. Rubler S, Dlugash J, Yuceoglu YZ, Kumral T, Branwood AW, Grishman A: New type of cardiomyopathy associated with diabetic glomerulosclerosis. *Am J Cardiol* 30:595–602, 1972
2. Hamby RI, Zoneraich S, Sherman L: Diabetic cardiomyopathy. *JAMA* 229:1749–1754, 1974
3. Regan TJ, Lyons MM, Ahmed SS, Levinson GE, Oldewurtel HA, Ahmad MR, Haider B: Evidence for cardiomyopathy in familial diabetes mellitus. *J Clin Invest* 60:884–899, 1977
4. Kannel WB, Hjortland M, Castelli WP: Role of diabetes in congestive heart failure: the Framingham study. *Am J Cardiol* 34:29–34, 1974
5. Bell DS: Diabetic cardiomyopathy. A unique entity or a complication of coronary artery disease? (Review) *Diabetes Care* 18:708–714, 1995
6. Baynes JW: Role of oxidative stress in development of complications in diabetes (Review). *Diabetes* 40:405–412, 1991
7. Low PA, Nickander KK, Tritschler HJ: The roles of oxidative stress and antioxidant treatment in experimental diabetic neuropathy. *Diabetes* 46 (Suppl. 2):S38–S42, 1997
8. Nishikawa T, Edelstein D, Du XL, Yamagishi S, Matsumura T, Kaneda Y, Yorek MA, Beebe D, Oates PJ, Hammes HP, Giardino I, Brownlee M: Normalizing mitochondrial superoxide production blocks three pathways of hyperglycaemic damage. *Nature* 404:787–790, 2000
9. Eriksson UJ, Borg LA: Diabetes and embryonic malformations: role of substrate-induced free-oxygen radical production for dysmorphogenesis in cultured rat embryos. *Diabetes* 42:411–419, 1993
10. Wolff SP, Jiang ZY, Hunt JV: Protein glycation and oxidative stress in diabetes mellitus and ageing. *Free Radic Biol Med* 10:339–352, 1991
11. Chen Y, Saari JT, Kang YJ: Weak antioxidant defenses make the heart a target for damage in copper-deficient rats. *Free Radic Biol Med* 17:529–536, 1994
12. Kaul N, Siveski-Iliskovic N, Hill M, Khaper N, Seneviratne C, Singal PK: Probucol treatment reverses antioxidant and functional deficit in diabetic cardiomyopathy. *Mol Cell Biochem* 42:283–288, 1996
13. Nishio Y, Kashiwagi A, Taki H, Shinozaki K, Maeno Y, Kojima H, Maegawa H, Haneda M, Hidaka H, Yasuda H, Horiike K, Kikkawa R: Altered activities of transcription factors and their related gene expression in cardiac tissues of diabetic rats. *Diabetes* 47:1318–1325, 1998
14. Wohaieb SA, Godin DV: Alterations in tissue antioxidant systems in the spontaneously diabetic (BB Wistar) rat. *Can J Physiol Pharmacol* 65:2191–2195, 1987
15. Wohaieb SA, Godin DV: Alterations in free radical tissue-defense mechanisms in streptozocin-induced diabetes in rat: effects of insulin treatment. *Diabetes* 36:1014–1018, 1987
16. Maulik N, Sharma HS, Das DK: Induction of the haem oxygenase gene expression during the reperfusion of ischemic rat myocardium. *J Mol Cell Cardiol* 28:1261–1270, 1996
17. Rosen P, Ballhausen T, Bloch W, Addicks K: Endothelial relaxation is disturbed by oxidative stress in the diabetic rat heart: influence of tocopherol as antioxidant. *Diabetologia* 38:1157–1168, 1995
18. Karasu C, Ozansoy G, Bozkurt O, Erdogan D, Omeroglu S: Antioxidant and triglyceride-lowering effects of vitamin E associated with the prevention of abnormalities in the reactivity and morphology of aorta from streptozotocin-diabetic rats: Antioxidants in Diabetes-Induced Complications (ADIC) Study Group. *Metabolism* 46:872–879, 1997
19. Naruszewicz M, Carew TE, Pittman RC, Witztum JL, Steinberg D: A novel mechanism by which probucol lowers low density lipoprotein levels demonstrated in the LDL receptor-deficient rabbit. *J Lipid Res* 25:1206–1213, 1984
20. Epstein PN, Overbeek PA, Means AR: Calmodulin-induced early-onset diabetes in transgenic mice. *Cell* 58:1067–1073, 1989
21. Kang YJ, Chen Y, Yu A, Voss-McCowan M, Epstein PN: Overexpression of metallothionein in the heart of transgenic mice suppresses doxorubicin cardiotoxicity. *J Clin Invest* 100:1501–1506, 1997
22. Overbeek PA, Aguilar-Cordova E, Hanten G, Schaffner DL, Patel P, Lebovitz RM, Lieberman MW: Coinjection strategy for visual identification of transgenic mice. *Transgenic Res* 1:31–37, 1991
23. Voss-McCowan ME, Xu B, Epstein PN: Insulin synthesis, secretory competence, and glucose utilization are sensitized by transgenic yeast hexokinase. *J Biol Chem* 269:15814–15818, 1994
24. Liang Q, Carlson EC, Borgerding AJ, Epstein PN: A transgenic model of acetaldehyde overproduction accelerates alcohol cardiomyopathy. *J Pharmacol Exp Ther* 291:766–772, 1999
25. Karnovsky MJ: A formaldehyde-glutaraldehyde fixitive for high osmolality for use in electron microscopy. *J Cell Biol* 35:137A–138A, 1965
26. Carlson EC, Hinds D: Native banded collagen fibrils in the glomerular mesangial matrix of normal human and laboratory animals. *J Ultrastruct Res* 77:241–247, 1981
27. Venable JH, Coggeshall R: A simplified lead stain for use in electron microscopy. *J Cell Biol* 25:407–408, 1965
28. Abel ED, Kaulbach HC, Tian R, Hopkins JC, Duffy J, Doetschman T, Minnemann T, Boers ME, Hadro E, Oberste-Berghaus C, Quist W, Lowell BB, Ingwall JS, Kahn BB: Cardiac hypertrophy with preserved contractile function after selective deletion of GLUT4 from the heart. *J Clin Invest* 104:1703–1714, 1999
29. Dutta K, Podolin DA, Davidson MB, Davidoff AJ: Cardiomyocyte dysfunction in sucrose-fed rats is associated with insulin resistance. *Diabetes* 50:1186–1192, 2001
30. Takeshita M, Ina K, Kitamura H, Shimada T, Nakamura M: Ultrastructural study of capillary and myocytic changes in the masseter and heart of KK-Ay mice. *J Electron Microsc* (*Tokyo*) 46:413–423, 1997
31. Malhotra A, Sanghi V: Regulation of contractile proteins in diabetic heart. *Cardiovasc Res* 34:34–40, 1997
32. Ye G, Ren J, Epstein PN: Metallothionein protects cardiomyocytes from diabetic damage (Abstract). *Diabetes* 50 (Suppl. 2):A171, 2001
33. Feuvray D, Idell-Wenger JA, Neely JR: Effects of ischemia on rat myocardial function and metabolism in diabetes. *Circ Res* 44:322–329, 1979
34. Seymour AM, Chatham JC: The effects of hypertrophy and diabetes on cardiac pyruvate dehydrogenase activity. *J Mol Cell Cardiol* 29:2771–2778, 1997
35. Doevendans PA, Daemen MJ, de Muinck ED, Smits JF: Cardiovascular phenotyping in mice. *Cardiovasc Res* 39:34–49, 1998
36. Kass DA, Hare JM, Georgakopoulos D: Murine cardiac function: a cautionary tail. *Circ Res* 82:519–522, 1998
37. Georgakopoulos D, Mitzner WA, Chen CH, Byrne BJ, Millar HD, Hare JM, Kass DA: In vivo murine left ventricular pressure-volume relations by miniaturized conductance micromanometry. *Am J Physiol* 274:H1416–H1422, 1998
38. Yuan SY, Ustinova EE, Wu MH, Tinsley JH, Xu W, Korompai FL, Taulman AC: Protein kinase C activation contributes to microvascular barrier dysfunction in the heart at early stages of diabetes. *Circ Res* 87:412–417, 2000
39. Spector KS: Diabetic cardiomyopathy. *Clin Cardiol* 21:885–887, 1998
40. Zhou Z, Kang YJ: Immunocytochemical localization of metallothionein and its relation to doxorubicin toxicity in transgenic mouse heart. *Am J Pathol* 156:1653–1662, 2000
41. Fiordaliso F, Li B, Latini R, Sonnenblick EH, Anversa P, Leri A, Kajstura J: Myocyte death in streptozotocin-induced diabetes in rats in angiotensin II-dependent. *Lab Invest* 80:513–527, 2000
42. Frustaci A, Kajstura J, Chimenti C, Jakoniuk I, Leri A, Maseri A, Nadal-

Ginard B, Anversa P: Myocardial cell death in human diabetes. *Circ Res* 87:1123–1132, 2000
43. Mak DH, Ip SP, Li PC, Poon MK, Ko KM: Alterations in tissue glutathione antioxidant system in streptozotocin-induced diabetic rats. *Mol Cell Biochem* 162:153–158, 1996
44. Ewis SA, Abdel-Rahman MS: Effect of metformin on glutathione and magnesium in normal and streptozotocin-induced diabetic rats. *J Appl Toxicol* 15:387–390, 1995
45. Sato M, Bremner I: Oxygen free radicals and metallothionein. *Free Radic Biol Med* 14:325–337, 1993
46. Lazo JS, Kuo SM, Woo ES, Pitt BR: The protein thiol metallothionein as an antioxidant and protectant against antineoplastic drugs (Review). *Chem Biol Interact* 111–112:255–262, 1998
47. Kumari MV, Hiramatsu M, Ebadi M: Free radical scavenging actions of metallothionein isoforms I and II. *Free Radic Res* 29:93–101, 1998
48. Miura T, Muraoka S, Ogiso T: Antioxidant activity of metallothionein compared with reduced glutathione. *Life Sci* 60:PL 301–309, 1997
49. Wang GW, Schuschke DA, Kang YJ: Metallothionein-overexpressing neonatal mouse cardiomyocytes are resistant to H2O2 toxicity. *Am J Physiol* 276:H167–H175, 1999